IOPscience iopscience.iop.org

Home Search Collections Journals About Contact us My IOPscience

An infrared study on the scattering mechanism in HgSe:Fe

This article has been downloaded from IOPscience. Please scroll down to see the full text article.

1991 J. Phys.: Condens. Matter 3 2693

(http://iopscience.iop.org/0953-8984/3/16/008)

View the table of contents for this issue, or go to the journal homepage for more

Download details:
IP Address: 171.66.16.151
The article was downloaded on 11/05/2010 at 07:12

Please note that terms and conditions apply.

J. Phys.: Condens. Matter 3 (1991) 2693–2702. Printed in the UK

An infrared study on the scattering mechanism in HgSe:Fe

Qian Dingrong†, Zhang Jiaming†, W Szuszkiewicz‡ and A Mycielski§

† National Laboratory for Infrared Physics, Academia Sinica, 420 Zhong Shan Bei Yi Road, Shanghai 200083, People's Republic of China

‡ Institute of Experimental Physics, Warsaw University, Hoza 69, 00-681 Warsaw, Poland

§ Institute of Physics, Polish Academy of Science, Al. Lotnikow 32/46, 02-668 Warsaw, Poland

Received 27 February 1990, in final form 2 January 1991

Abstract. The infrared absorption and reflectivity of HgSe:Fe samples with Fe concentrations ranging from 1.5×10^{18} to 7×10^{19} cm^{-3} have been investigated at room temperature in the region 400–2000 cm^{-1}. The Drude theory modified with a frequency-dependent damping and the Γ_8^v–Γ_8^c interband contribution as well as the general theory of free-carrier absorption which takes into account both single-particle and collective absorptions were employed to study the experimental results. The spectral data enable the evaluation of material parameters, such as E_F, N_e, m_l^* and m_s^*, as well as the determination of the damping parameter, absorption coefficient, absorption cross section and mobility. It was found unexpectedly that the absorption parameters and mobility undergo an evident change in their dependence on Fe concentration when the Fe concentration is higher than 4×10^{18} cm^{-3}; a weakened scattering rate on free carriers has been assumed.

1. Introduction

$Hg_{1-x}Fe_xSe$ is a relatively new semimagnetic semiconductor which has attracted considerable attention owing to its many interesting and novel properties. HgSe is a zero-gap semiconductor with inverted energy band structure similar to that proposed by Groves and Paul [1, 2] for α-Sn. Fe in HgSe acts as a resonant donor. The ground state of Fe^{2+} $3d^6$ impurities is split by the tetrahedral crystal field into a ^5E orbital and higher-lying ^5T orbital triplet. Both of them are degenerate with the conduction band [3–5]. It is believed that the ^5E term is located at 210 meV above the bottom of the band while the ^5T term lies about 370 meV higher. Our previous investigation [6] on the infrared properties of HgSe:Fe sample with a Fe concentration of 7×10^{18} cm^{-3} showed that at temperatures below 20 K the Fermi level is pinned to ^5E, which is not greater than 200 meV above the bottom of conduction band, and increases with temperature owing to the depopulation of Fe^{2+}. The recent investigations of $Hg_{1-x}Fe_xSe$ have revealed that this system shows a strikingly different behaviour from that found in HgSe and $Hg_{1-x}Mn_xSe$ at low temperatures when the Fe concentration is greater than a critical value which is about $(4–5) \times 10^{18}$ cm^{-3}. Among these different properties are the very stable electron concentration [7], the apparent reduction in Dingle temperature and the unusually high electron mobility [5, 8–12]. To explain these striking features, a spatial

0953-8984/91/162693 + 10 $03.50 © 1991 IOP Publishing Ltd

ordering model of charges within the ionized donor of the Fe system through Coulomb interactions was examined by Mycielski [13]. According to this model, the space ordering of the ionized donor, which takes place at low temperatures when the concentration of Fe exceeds this critical concentration, appreciably reduces the carrier scattering rate and hence results in the novel properties. Similarly, the scattering of carriers by charged centres should also substantially affect the intraband transition of free carriers from the view that free carriers have to exchange their momentum with lattice through scattering in order to be excited into a higher state of energy in the process of intraband optical absorption.

This paper is an optical study of the influence of Fe ions in HgSe on the scattering mechanism of free carriers in the infrared region.

2. Absorption and reflectivity

Infrared transmission and reflectivity measurements of crystalline HgSe:Fe samples obtained using Bridgman method with a doping concentration of Fe in the range 1.5×10^{18}–$7 \times 10^{19}\,\mathrm{cm}^{-3}$ have been performed. A Perkin–Elmer 983 grating spectrometer and a Brucker IFS-113V Fourier spectrometer were used for the measurements in the spectral range 400–2000 cm^{-1}. Firstly, the reflectivity was measured. The thickness of samples is about 0.5 mm, which is thick enough that the influence of the second surface can be neglected; then the samples were reduced to the thickness of 10–50 μm and glued on a ZnS or sapphire substrate with a hole at the centre for the transmission measurement. The measurements were performed with a special effort to extend the measuring region as close as possible to plasma edge so as to obtain free-carrier absorption in a wide range of frequencies. The samples were prepared by mechanical polishing followed by etching in 4% bromine–methanol solution. A 'transmission window' with Fe-dependent width and position is observed.

The measured reflectivity spectra were fitted using

$$R = [(n-1)^2 + k^2]/[(n+1)^2 + k^2] \tag{1}$$

$$n = \sqrt{(\sqrt{\varepsilon_1^2 + \varepsilon_2^2} + \varepsilon_1)/2} \qquad k = \sqrt{(\sqrt{\varepsilon_1^2 + \varepsilon_2^2} - \varepsilon_1)/2} \tag{2}$$

where n is refractive index, k is the extinction coefficient, and ε_1 and ε_2 are the frequency-dependent real and imaginary parts, respectively, of the complex dynamic dielectric function (DDF). The DDF for a zero-gap semiconductor is given by the general formula

$$\varepsilon(\omega) = \varepsilon_1(\omega) + \mathrm{i}\varepsilon_2(\omega) = \varepsilon'_\infty + \varepsilon_{\mathrm{inter}}(\omega) + \varepsilon_{\mathrm{ph}}(\omega) + \varepsilon_{\mathrm{intra}}(\omega)$$

$$= \varepsilon_\infty(\omega) + \varepsilon_{\mathrm{intra}}(\omega) \tag{3}$$

$$\varepsilon_{\mathrm{ph}}(\omega) = F\omega_{\mathrm{TO}}^2/(\omega_{\mathrm{TO}}^2 - \omega^2) \tag{4}$$

$$\varepsilon_{\mathrm{intra}}(\omega) = -\omega_{\mathrm{p}}^2/(\omega^2 - \mathrm{i}\gamma\omega) \tag{5}$$

where ω_{p} is the plasma frequency, γ the damping parameter, ω_{TO} the transverse optical phonon frequency and F the oscillator strength. The weak phonon damping has been neglected. ε'_∞ is the contribution due to all interband transition except the Γ_8^v–Γ_8^c transition $\varepsilon_{\mathrm{inter}}(\omega)$. $\varepsilon_{\mathrm{inter}}(\omega)$ can be calculated using two band-structure models: the 'quasi-parabolic' model and the model of Kane with large spin–orbit splitting and random-phase approximation [14, 15]. The parameters used in this calculation are the

same as in [15]. The integral in the calculation of DDF was divided into two parts: one for the energy at which the shape of the band is described by Kane's model, and the second for the energy range in which a damping function proposed first by Stern [16] was employed, where the two parameters used in the function are $E_1 = 1.0$ eV and $E_s = 3.0$ eV. Our evaluation shows that $\varepsilon_{inter}(\omega)$ has a relatively flat dispersion relation at room temperature. ε'_∞ is taken to be a frequency-independent fitting constant in this study. Strictly speaking, ε'_∞ is frequency dependent at a frequency corresponding to the Fermi energy. In fact, at room temperature, there is almost no such contribution because of the minor density of states in the Γ_6^v valence band. However, it was found from the fitting that ε'_∞ is Fe concentration dependent, a result which has not been reported before and is perhaps associated with the position of the Fermi level in the conduction band. ω_p and γ are fitting parameters also. Using the DDF in equations (1) and (2), one can attain a very good fit to the measured reflectivity. The parameters obtained are listed in table 1. The absorption coefficient α can then be obtained from the transmission T:

$$T = [(1 - R)^2/(1 - R^2)] \exp(-\alpha d). \tag{6}$$

The thickness d was determined from the interference in the transmission spectrum using the refractive index n calculated from equation (2). In figure 1 are the absorption coefficients thus obtained for five samples in a typical free-carrier absorption region, which ends at the plasma frequency ω_p on the low-wavenumber side. In the same plot are also shown the absorption coefficients evaluated from the damping parameters through equations (5), (3) and (2):

$$\alpha = 4\pi k/\lambda \tag{7}$$

where λ is the wavelength. The coincidence between the fits to the Drude theory and experiment is very good. It is obvious that the absorption does not increase with increasing Fe concentration constantly. When the Fe concentration increases by a factor of 2.7 (from 1.5×10^{18} to 4×10^{18}), the absorption coefficient increases by a factor of 2.3, which is, roughly speaking, proportional to the Fe concentration, and then for a further increase in Fe by a factor as large as 17.5 (from 4×10^{18} to 7×10^{19}) the absorption coefficient remains at about the same level. It follows from this that the absorption of light by HgSe:Fe becomes less effective when the Fe concentration is higher than the critical concentration.

The dependence $\alpha \sim \lambda^s$ of the absorption coefficient on wavelength has been studied by power-law regression on the linear part of the curves in figure 1; $s = 3.5$ and 2.5 indicate ionized-impurity and phonon scattering mechanisms for samples with Fe concentrations higher than 4×10^{18} cm^{-3} and equal to or less than 4×10^{18} cm^{-3}, respectively. Our previous study on free-carrier absorption in $Hg_xCd_{1-x}Te$ [17] revealed 3.7 and 2.7 wavelength power dependences of the absorption coefficient for ionized-impurity and phonon scattering, respectively (in that paper, the power dependence of 3.7 and 2.7 was erroneously printed as 1.0 and 1.4, respectively). Therefore, when the total concentration of Fe in the crystal exceeds the critical value and the predominant scattering mechanism turns out to be ionized-impurity scattering created mainly by Fe^{3+} $3d^5$, the absorption no longer increases. However, the density of free carriers increases steadily with increasing Fe concentration (table 1); it is then concluded that the scattering rate of free carriers on Fe^{3+} decreasingly becomes less effective when the Fe concentration exceeds the critical value.

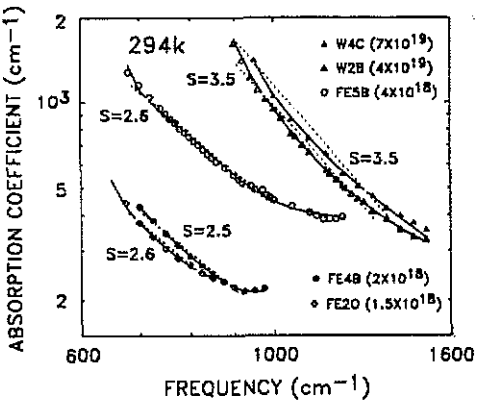

Figure 1. Absorption coefficient versus frequency: ▲, △, ○, ●, ◇, experimental data; ——, theoretical values from the Drude theory; – – –, linear regression to the linear part of the experimental data. The *s*-values are the slope of the linear regression line with respect to frequency in the linear part.

Table 1. The parameters for five samples: N_{Fe} is a material parameter, d is a sample parameter, ω_p and $\varepsilon_\infty(\omega_p)$ are fitting parameters, E_F is a parameter calculated from the fitting parameters, and N_e, m_l^* and m_s^* are parameters calculated from E_F.

Sample	N_{Fe} (10^{18} cm^{-3})	d (μm)	ω_p (cm^{-1})	$\varepsilon_\infty(\omega_p)$	S	N_e (10^{18} cm^{-3})	E_F (meV)	m_l^* (units of m_0)	m_s^* (units of m_0)
FE2O	1.5	49.5	610	12.0	2.6	2.1	257	0.040 07	0.042 86
FE4B	2	55.4	630	11.9	2.5	2.3	266	0.041 13	0.043 84
FE5B	4	13.75	650	11.8	2.6	2.5	273	0.042 17	0.044 81
W2B	40	21.4	830	11.6	3.5	4.9	352	0.052 56	0.054 62
W4C	70	21.5	860	11.1	3.5	5.1	357	0.053 22	0.055 26

3. Damping parameter

It was found that γ is an insensitive parameter in reflectivity fitting using equation (1) except for the region close to the plasma frequency. On the contrary, it is very sensitive in the fitting to the measured absorption coefficients using equations (5), (3), (2) and (7), and the fitting is not satisfactory unless a frequency-dependent damping is used in equation (5). In fact, a square-law frequency-dependent damping has already been employed by other workers in their optical analysis of semiconductors [18–20] and metals [21] and was believed to be associated with plasmon generation [22]. It is seen from figure 2 that damping in the three lower-Fe-concentration samples is more frequency dependent than that in the two high-Fe-concentration samples. Figure 3 presents the tendency of the variation in damping parameter with Fe concentration. It is also seen that damping increases proportionally with increasing concentration of Fe if it is less than the critical value; then the damping does not undergo any noticeable increase for further increase in Fe.

4. Absorption cross section

The plasma frequency is given by

$$\omega_p^2 = 4\pi N_e e^2/\varepsilon_\infty(\omega_p)m_s^* \tag{8}$$

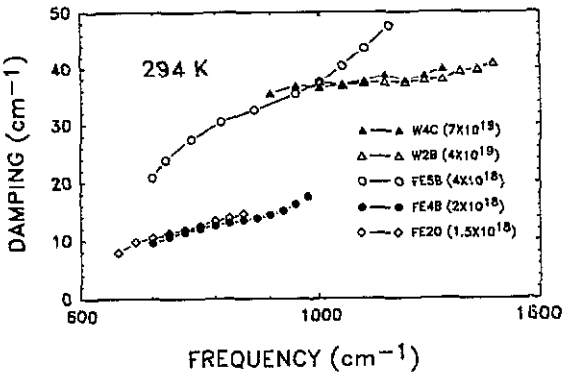

Figure 2. Damping parameter versus frequency.

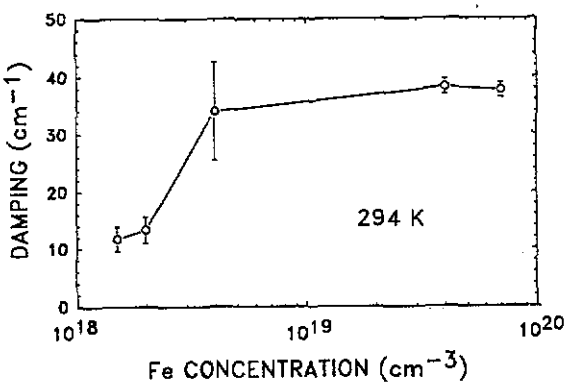

Figure 3. The mean value of damping parameter averaged over the linear region of free-carrier absorption versus Fe concentration. The error bars indicate the derivative of the data in the region. The full line is a guide to the eye.

where e is the charge of electron, N_e is the density of free electrons $\varepsilon_\infty(\omega_p)$ is the sum of $\varepsilon'_\infty + \varepsilon_{inter}(\omega) + \varepsilon_{ph}(\omega)$ at the frequency ω_p at which the real part of DDF goes to zero, m_s^* is the effective mass of free carriers averaged over the conduction band: $m_s^* = \langle m_c^* \rangle$ [23, 24]. The angular brackets signify an average over the distribution and this average is defined, for the case of spherical constant-energy surface, by

$$\langle A \rangle = \left[\int_0^\infty \left(-\frac{\partial f}{\partial E}\right) Ak^3 \, dE\right] \Big/ \left[\int_0^\infty \left(-\frac{\partial f}{\partial E}\right) k^3 \, dE\right] \tag{9}$$

where f is the Fermi–Dirac distribution function, and k the wavevector. ε'_∞ and $\varepsilon_\infty(\omega_p)$ can then be obtained from reflectivity fitting using equations (1)–(3). Moreover, since both N_e and m_s^* in equation (8) are functions of the Fermi energy E_F, the accurate values of E_F can then be evaluated by the method of successive approximations to the measured ω_p. Table 1 presents the evaluated N_e, m_s^* and m_t^* for five samples; the values of N_e are less than those from Hall measurement [5]. Recently, a method of evaluating E_F from the interband transition edge using the imaginary part of DDF was proposed [6]; the obtained value of E_F is slightly less than that shown in table 1. With the values of N_e in

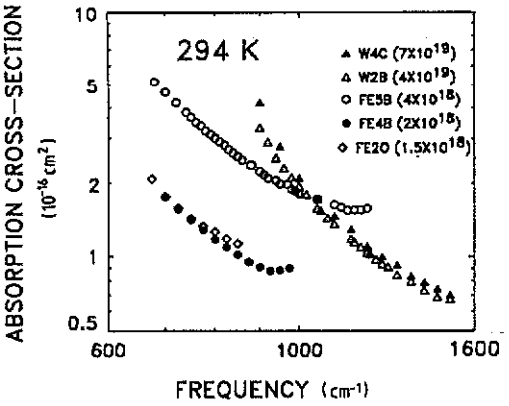

Figure 4. Absorption cross section versus frequency. The value of the density of free carriers is evaluated from the plasma frequency.

table 1, the absorption cross sections (figure 4) were evaluated from the absorption coefficients (figure 1) for the five samples. A similar tendency is demonstrated once again that an obvious increase is followed by a slow decrease. This demonstrates clearly the strengthening and weakening in the scattering rate of free carriers.

5. Mobility

The high-frequency mobility was evaluated from the damping parameter γ and the effective mass m_f^* of free carriers at E_F by

$$\mu = e/2\pi c m_f^* \gamma \tag{10}$$

where c is the velocity of light. The results are presented in figure 5. It is seen that the mobility is both frequency and Fe concentration dependent for samples with a Fe concentration less than the critical value; also it turns out to be frequency and Fe concentration independent and has lower value for samples with a Fe concentration higher than the critical value. Figure 6 is the plot of mobility versus Fe concentration.

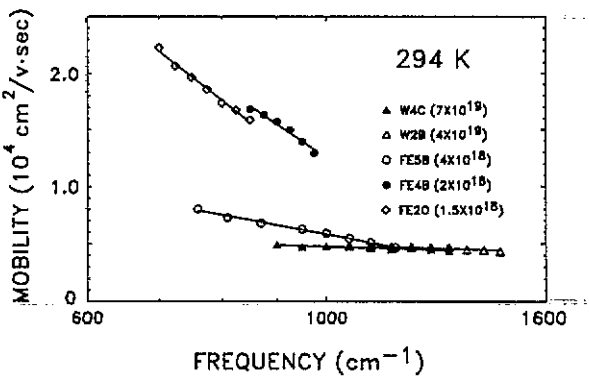

Figure 5. High-frequency mobility evaluated from damping parameter versus frequency. The full line is a guide to the eye.

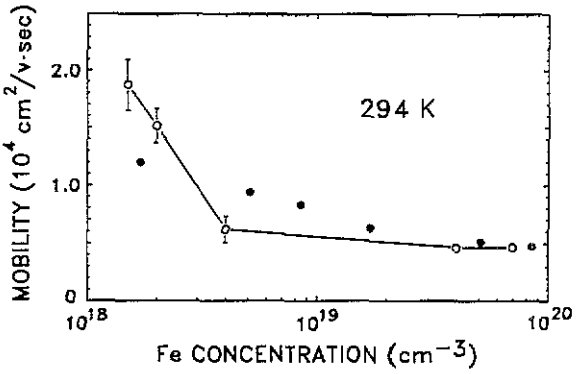

Figure 6. Mobility versus Fe concentration: ○, mean values of high-frequency mobility (the error bars indicate the derivative of the data; the full line is a guide to the eye); ●, static mobility from [5].

The mobility decreases with increasing Fe concentration, but the decreasing rate undergoes an obvious change at the critical value of Fe concentration. The static mobility obtained from transport measurements [5] is also shown in figure 6. It decreases with no turning point and approaches the high-frequency mobility in the high-Fe-concentration region. Figure 7 is the plot of mobility versus free-carrier density. The trend is the same as that in figure 6. The turning point in figure 7 at about 2.5×10^{18} cm^{-3} is determined by the critical value of Fe concentration. A weakened scattering rate of free carriers, which starts at the turning point, is an easy interpretation for the trend.

6. Discussion

Although the theoretical plots in figure 1 based upon the modified Drude theory describe the free-carrier absorption in HgSe:Fe very well, this theory is essentially classical; it fails to give detailed description of the specific scattering mechanisms. In order to

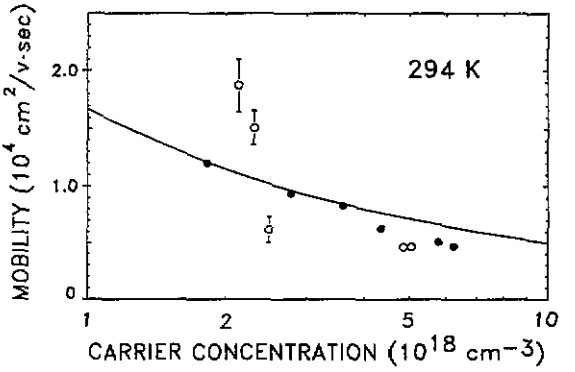

Figure 7. Mobility versus density of free carriers: ○, mean values of high-frequency mobility (the error bars indicate the derivative of the data); ◐, static mobility from [5]; ——, theoretical value from [25].

calculate the intraband free-carrier absorption coefficient due to varied scattering mechanisms, a modified quantum theory and a photon-ionized-impurity-plasmon (PIIP) process were employed in our previous studies [17, 26] to account for the two parts of the free-carrier absorption, i.e. that due to single-carrier transitions and that due to collective excitations of free carriers. However, the PIIP process does not take into consideration the damping of plasmon oscillations so that it overestimates the effect due to plasmon excitations in the high-frequency region where Landau damping exists. The more general theory of high-frequency free-carrier absorption due to impurity scattering at absolute zero temperature for an n-type doped zero-gap semiconductor with parabolic and isotropic Γ_8^+ conduction band has been put forward by Goettig [27]. In the theory, both single-particle absorption and collective absorption are evaluated for the degenerate plasma, and also in the frequency range corresponding to the Landau damped collective modes. In addition, the plasma–LO-phonon polar coupling is taken into account in the theory. With this theory, a very good description of the low-temperature transmission data of HgSe has been obtained [27]. According to this theory, we have numerically evaluated $\mathrm{Im}[\alpha^{\delta}(\omega)]$, i.e. the total dissipative parts of intraband polarizability which is the contribution to DDF due to the interactions of free carriers with ionized impurities in the lattice. The parameters used in this study are the same as used by Goettig. Material parameters such as N_e, E_F, m_s^* and ω_p are listed in table 1. It was assumed in the theory that the scatterers, i.e. ionized Fe donors, are distributed at random and $D = (1/N_e)\,\Sigma_i Z_i^2 N_i$, where N_e is free carrier density and i represents the different kinds of impurity, while Z_i and N_i denote the charge number and the concentration of impurities of the i kinds of impurity, respectively. A D-value higher than unity indicates either a large charge number on the scatterers, which is not the case for Fe ions in HgSe, or a higher concentration of scatterers with respect to N_e. Since the samples are highly degenerate, the free-carrier behaviour at a finite temperature should not be very different from that at absolute zero temperature, so that we can use this theory to estimate our results. The absorption coefficient can be calculated from

$$\alpha = (4\pi\omega/cn)\,\mathrm{Im}[\alpha^{\delta}(\omega)]. \tag{11}$$

Figure 8 shows the evaluated results as well as the D-values used in the calculations. The slopes of all curves are the same and are around 3.5 which is typical for ionized-impurity scattering. The agreement between theory and experiment is good for samples W4C and W2B. It is very interesting to compare the increase in D-value with that in Fe

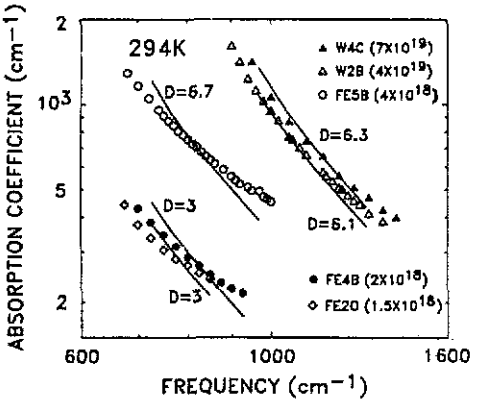

Figure 8. Absorption coefficient versus frequency: ▲, △, ○, ●, ◇, experimental values; ——, theoretical values from [27]. The D-values are the impurity parameter.

concentration. For sample FE5B, the Fe concentration is 2.0 and is 2.6 times that in samples FE4B and FE2O, while its D-value is 2.2 times that for the two samples. The predominant scattering mechanism in these three samples is, as we have pointed out, phonon scattering. Fitting the measured absorption coefficients using Goettig's theory which takes into account only ionized-impurity scattering has certainly overestimated the D-value. However, the relative increase in D-value still makes sense, indicating the increase in ionized impurities. On the other hand, for samples W4C and W2B, their Fe concentrations are 10.0 and 17.5 times that for sample FE5B while their D-values are only 0.9 times that for sample FE5B, indicating no extra increase in ionized impurities with respect to free carriers.

The electron scattering in crystals such as HgSe is rather complicated owing to the peculiar order of the energy levels which causes several specific problems in the theory. In particular, the formulae derived in the past for an s-type band cannot be directly applied to materials with an inverted band structure. Dietl and Szymanska [25] and Szymanska and Dietl [28] have developed a theory of electron scattering and transport phenomena taking into consideration many specific features of electron transport in the band in question for a randomly distributed assembly of scatterers. The full curve in figure 7 is the result obtained from their theory in which the contributions from ionized-impurity, polar, acoustic and non-polar scattering have been taken into consideration. For comparison, the static mobility from [5] is plotted also. The theory describes the static mobility well in the region of low carrier density but not in the region of high carrier density where the static mobility is less than theory and approaches the high-frequency mobility. As far as the high-frequency mobility is concerned, this theory fails to describe it in both trend and value.

The scattering relaxation time has also been evaluated from Goettig's theory; it is seen that the scattering frequency for the five samples are of the order of magnitude of 10^{11}–10^{12} Hz, while the optical frequency in this study is of the order of 10^{13} Hz, which is one or two orders of magnitude higher than scattering frequency. Thus the two mobilities, from optical and transport measurement, should not be the same. A study on rather pure HgTe samples [14] showed that the dynamic damping obtained from room-temperature reflectivity fitting is about 50% greater than static damping obtained from Hall mobility; in other words, the high-frequency mobility should be 50% less than the static mobility. It is seen from figure 7 that this is not the case.

It follows then that the scattering theory based upon the random distribution of ionized impurities is no longer accurate in the case of HgSe:Fe.

It was suggested that $Hg_{1-x}Fe_xSe$ can contain microscopic Hg inclusions [29]. It is then very likely to have HgSe surrounded by Hg inclusions in the lattice; these inclusions have an effect on the transmission spectrum depending on their density and size distribution, and the effect is hard to distinguish from those due to free-carrier absorptions. The situation is similar to that arising from HgTe inclusions in $Hg_xCd_{1-x}Te$ [30]. The effect of HgTe inclusions in the $Hg_{1-x}Cd_xTe$ lattice on infrared transmission is temperature sensitive; HgSe inclusions are expected to have the same temperature behaviour. Therefore, low-temperature investigations of HgSe:Fe are needed.

7. Conclusion

When the Fe concentration in HgSe:Fe increases to a value higher than the critical value, the scattering rate of free carriers on the resonant donors Fe^{3+} is weakened; this

results in an obvious change in the dependence of absorption coefficient, damping parameter, absorption cross section and mobility on Fe concentration. Neither the high-frequency mobility nor the static mobility in the region of high free-carrier density can be described by the existing free-carrier scattering theory which is based upon a random distribution of ionized impurities. The two mobilities (dynamic and static) have the same value when the density of free carriers and hence the Fe concentration is high enough. All the results in this study indicate that free-carrier scattering is weakened when the total Fe concentration is higher than the critical value.

Acknowledgments

The assistance of Ji Huamei, Liu Kun, Huang Yexiao and Hu Canming in the preparation and performance of this experiment is appreciated. Thanks are also due to Mrs B Witkowska for providing us with the HgSe:Fe crystals.

References

[1] Groves S H and Paul W 1963 *Phys. Rev. Lett.* **11** 194
[2] Groves S H and Paul W 1964 *Proc. Int. Conf. on Semiconductors* (Paris: Dunod) p 41
[3] Mycielski A, Kowalski B, Orlowski B A, Dobrowlska M, Arciszewska M, Dobrowolski W and Baranowski J M 1986 *J. Phys. C: Solid State Phys.* **19** 3605
[4] Mycielski A 1988 *J. Appl. Phys.* **63** 3279
[5] Pool F S, Kossut J, Debska U and Reifenberger R 1987 *Phys. Rev.* B **35** 3900
[6] Szuszkiewicz W, Qian Dingrong, Julien C, Zhang Jiaming, Jezewski M, Balkanski M and Mycielski A 1990 *J. Cryst. Growth* **101** 507
[7] Vaziri A, Debska U and Reifenberger R 1985 *Appl. Phys. Lett.* **47** 407
[8] Vaziri A and Reifenberger R 1985 *Phys. Rev.* B **32** 3291
[9] Vaziri A and Reifenberger R 1986 *Phys. Rev.* B **33** 5585
[10] Reifenberger R and Kossut J 1987 *J. Vac. Sci. Technol.* A **5** 2995
[11] Dobrowolski W, Dybko K, Mycielski A, Mycielski J, Piechota S, Palczewska M, Szymczak H and Wilamowski Z 1986 *Proc. 18th Int. Conf. on the Physics of Semiconductors (Stockholm 1986)* ed O Engstrom (Singapore: World Scientific) p 1743
[12] Glutzman N G, Sabirzyanova L D, Tsidil'kovskii I M, Paranchich L D and Paranchich S Yu 1986 *Fiz. Tekh. Poluprov.* **20** 1994
[13] Mycielski J 1986 *Acta Phys. Polon.* A **69**; 1986 *Solid State Commun.* **60** 165
[14] Grynberg M, Le Toullec R and Balkanski M 1974 *Phys. Rev.* **9** 517
[15] Szuszkiewicz W, Witowski A M and Grynberg M 1978 *Phys. Status Solidi* b **87** 637
[16] Stern F 1964 *Phys. Rev.* **133** A1653
[17] Qian Dingrong and Szuszkiewicz W 1987 *Phil. Mag. Lett.* **55** 147
[18] Kushev D B, Zheleva N N, Demakopoulou Y and Siapkas D 1986 *Infrared Phys.* **26** 385
[19] Gopal V 1982 *Infrared Phys.* **22** 237
[20] Paraskevopoulos K, Siapkas D and Economou N 1984 *Phys. Status Solidi* b **124** 229
[21] Thye M 1970 *Phys. Rev.* B **2** 3060
[22] Szuszkiewicz W and Witowski A M 1983 *Solid State Commun.* **48** 821
[23] Zawadzki W 1974 *Adv. Phys.* **23** 435
[24] Manabe A, Noguchi H and Mitsuishi A 1978 *Phys. Status Solidi* b **90** 157
[25] Dietl T and Szymanska W 1978 *J. Phys. Chem. Solids* **39** 1041
[26] Qian Dingrong, Tang Wenguo, Shen Jie, Chu Junhao and Zheng Guozhen 1985 *Solid State Commun.* **56** 813
[27] Goettig S 1985 *Solid State Commun.* **55** 611
[28] Szymanska W and Dietl T 1978 *J. Phys. Chem. Solids* **39** 1025
[29] Dietl T 1990 *J. Cryst. Growth* **101** 808
[30] Qian Dingrong 1986 *Phys. Status Solidi* a **94** 573